shift and strain scattering contributions turn out to be of comparable importance, then a larger relaxation may perhaps be permitted, due to the possibility of interference effects.

ACKNOWLEDGMENT

One of us (P. M. L.) wishes to acknowledge the award of an Ellison Fellowship by the University of Sheffield.

PHYSICAL REVIEW VOLUME 118, NUMBER 1 APRIL 1, 1960

Effects of Double Exchange in Magnetic Crystals*

P.-G. DE GENNES†
Department of Physics, University of California, Berkeley, California
(Received October 9, 1959)

This paper discusses some effects of mobile electrons in some antiferromagnetic lattices. It is shown that these electrons (or holes) always give rise to a distortion of the ground state spin arrangement, since electron transfer lowers the energy by a term of first order in the distortion angles. In the most typical cases this results in: (a) a nonzero spontaneous moment in low fields; (b) a lack of saturation in high fields; (c) simultaneous occurrence of "ferromagnetic" and "antiferromagnetic" lines in neutron diffraction patterns; (d) both ferromagnetic and antiferromagnetic branches in the spin wave spectra. Some of these properties have indeed been observed in compounds of mixed valency such as the manganites with low Mn^{4+} content. Similar considerations apply at finite temperatures, at least for the (most widespread) case where only the bottom of the carrier band is occupied at all temperatures of interest. The free energy is computed by a variational procedure, using simple carrier wave functions and an extension of the molecular field approximation. It is found that the canted arrangements are stable up to a well-defined temperature T_1. Above T_1 the system is either antiferromagnetic or ferromagnetic, depending upon the relative amount of mobile electrons. This behavior is not qualitatively modified when the carriers which are responsible for double exchange fall into bound states around impurity ions of opposite charge. Such bound states, however, will give rise to local inhomogeneities in the spin distortion, and to diffuse magnetic peaks in the neutron diffraction pattern. The possibility of observing these peaks and of eliminating the spurious spin-wave scattering is discussed in an Appendix.

I. INTRODUCTION

We are concerned here with magnetic compounds of mixed valency, of which the best known example is the series $(La_{1-x}Ca_x)(Mn_{1-x}^{3+}Mn_x^{4+})O_3$. At both ends of the composition diagram, these manganites behave like antiferromagnetic insulators.[1,2] However, to take a definite example, if we substitute 10% of calcium in pure $LaMnO_3$ the room temperature conductivity is increased by two orders of magnitude.[1] This shows that the 10% extra holes which have been added are comparatively free to move from one manganese ion to another, and are able to carry a current. These carriers also have a strong effect on the magnetic properties of the material: at low temperatures there is a nonzero spontaneous magnetization (approximately 0.4 of what is expected for complete lining up of the spins on the above example), indicating that some sort of ferromagnetic coupling is present. This was first explained by Zener[3] in the following way: (1) intra-atomic exchange is strong so that the only important configurations are those where the spin of each carrier is parallel to the local ionic spin; (2) the carriers do not change their spin orientation when moving; accordingly they can hop from one ion to the next only if the two ionic spins are not antiparallel; (3) when hopping is allowed the ground state energy is lowered (because the carriers are then able to participate in the binding). This results in a lower energy for ferromagnetic configurations. This "double exchange" is completely different from the usual (direct or indirect) exchange couplings, as pointed out by Anderson and Hasegawa.[4] The coupling energy is shared between the carriers, and cannot be written as a sum of terms relating the ionic spins by pairs. Also, the dependence of the carrier energy on the angle between different ionic spins is quite remarkable. This brings in special effects which do not seem to have been considered up to now. For instance, if the pure material is antiferromagnetic, it will turn out that the carrier energy in the mixed material is lowered if the sublattices become canted. This gain in energy is of first order with respect to the angle of canting, while the loss of antiferromagnetic exchange energy is only of second order; as a result, the canted arrangement is indeed more stable. It is the

* Supported by the National Science Foundation.
† On leave from the Centre d'Etudes Nucleaires de Saclay, Gif-sur-Yvette, France.
[1] G. H. Jonker and J. H. Van Santen, Physica **16**, 337 (1950); **19**, 120 (1953).
[2] E. O. Wollan and W. C. Koehler, Phys. Rev. **100**, 545 (1955).
[3] C. Zener, Phys. Rev. **82**, 403 (1951).
[4] P. W. Anderson and H. Hasegawa, Phys. Rev. **100**, 675 (1955).

purpose of this paper to discuss these distorted arrangements, especially as regards their stability and their effects on magnetic properties.

As a first step, we now outline the very simplified physical model which will be used in the calculations of the later sections. We shall describe the carrier wave functions, in a tight binding approximation, as a linear combination of some orthogonal functions φ_i localized on each magnetic site (i):

$$\psi=\sum\alpha_i\varphi_i. \tag{1}$$

The φ's are such that off-diagonal elements of the one-electron Hamiltonian between them and the anion orbitals are zero. The eigenvalue equation satisfied by the amplitudes α_i is then of the form

$$E\alpha_i=\sum_j t_{ij}\alpha_j \tag{2}$$

where $t_{ij}=(\varphi_i|\mathcal{H}|\varphi_j)$ is a matrix element of the one-carrier Hamiltonian $\mathcal{H}$, commonly referred to as the transfer integral between ions i and j. In practice t_{ij} connects only neighboring magnetic sites. When the ionic spins $\mathbf{S}_i$ and $\mathbf{S}_j$ are parallel, t_{ij} is maximum and equal to some constant b_{ij}. When $\mathbf{S}_i$ and $\mathbf{S}_j$ are antiparallel, $t_{ij}=0$. More generally, as shown in reference 4, when $\mathbf{S}_i$ makes an angle θ_{ij} with $\mathbf{S}_j$ the transfer integral for carriers of spin $\frac{1}{2}$ is

$$t_{ij}=b_{ij}\cos(\theta_{ij}/2). \tag{3}$$

Equations (1), (2), and (3) rely on the following simplifications: (a) the fivefold degeneracy of the d band is neglected; (b) the intra-atomic exchange integral is assumed larger than b_{ij} (so that transfer for $\theta_{ij}=\pi$ is indeed negligible); (c) the ionic spins $\mathbf{S}_i$ are described as classical vectors; (d) the ions are held rigidly at their equilibrium positions; (e) Coulomb interactions between carriers are not considered; (f) interactions between the carriers and the compensating charges of opposite sign (e.g., Ca^{++} substituted for La^{+++}) are averaged out. Removal of (a) would not qualitatively modify the considerations to be developed in the following but would only complicate matters by introducing more unknown parameters; (b) and (c) are good starting approximations in all cases; (d) neglects the strong coupling between carriers and lattice vibrations, the importance of which has been stressed by Zener.[5] However, we shall be interested only in the lowest energy levels of the carriers and only in the part of this energy which depends on the orientations of the ionic spins. It is then reasonable to treat the polaron self-energy as an additive constant, so that (d) is an acceptable assumption. On the other hand a study of effective masses and mobilities would require a more detailed treatment of the carrier-phonon interaction, so that we do *not* expect the b_{ij}'s to be simply related to the electrical conductivity. Assumption (e) restricts us to dilute carrier systems. Fortunately this is a mild requirement because double exchange effects are often strong even in this limit. Assumption (f) is a drastic simplification. It amounts to neglecting all possible bound states of the carriers around the impurities which have been used to create a state of mixed valency. One might argue that as soon as the conductivity of the mixed specimens is much larger than the conductivity of the pure material, a band picture is appropriate. However, this conductivity, although high, often shows a temperature dependence corresponding to an activation energy; we believe that for low concentrations only a small fraction of the Zener electrons is involved in the conduction process, while all of them (bound or not bound) participate in double exchange. The essential observation here is that the over-all effects of bound carriers on the ionic spins is in fact very similar to the effect of the free carriers described by Eq. (2), as will be shown in Sec. IV. (In both cases the carrier energy is lowered by a distortion of the ionic spin arrangement.) The magnetic properties of our assembly are not strongly affected by assumption (f), and our simple model is indeed applicable.

To study effects of thermal excitation it is very important to recognize that in many cases the over-all band width of the carriers is expected to be large when compared with the temperatures of interest. (From the transition temperatures in the manganite series we infer that the band width is at least $\sim$0.1 ev and probably larger.) This shows that the anomalies in paramagnetic behavior predicted by Anderson and Hasegawa,[4] which are due to a uniform filling of the band, cannot be observed in general. The opposite situation, where the carriers fill only the bottom of the band, is much closer to the actual state of affairs, and we shall deal uniquely with this limiting case. The behavior of the system at finite temperatures still remains an extremely complicated problem, and the difficulties are twofold: first, we have to know the ground state energy of the one-carrier Hamiltonian for all arrangements of the ionic spins. This is a question of wave propagation in a three-dimensional disordered medium, and can be solved only by means of very rough approximations. Second, there is the problem of the statistical behavior of the ionic spins submitted to the double exchange coupling. As we shall see in Sec. III, even the molecular field approach involves some labor in this instance, but, apart from these computational difficulties, we are able to get a clear picture of the successive transitions that occur. The major difficulty with which we are left is then due to the rather large number of interaction constants which have to be derived from experiment; for instance, when dealing with a "layer" antiferromagnet, we need both the intra-layer and inter-layer exchange couplings of the pure material, and the two corresponding transfer integrals, that is to say four constants. Possible means of deriving these constants are discussed in Sec. V.

[5] C. Zener, J. Phys. Chem. Solids 8, 26 (1959).

II. CANTED SPIN ARRANGEMENTS AT LOW TEMPERATURES

We now consider a Bravais lattice of magnetic ions, and further assume that the spin ordering of the unperturbed system is of the "*antiferromagnetic layer*" type. Each ionic spin of length S is coupled ferromagnetically to z' neighboring spins in the same layer, and antiferromagnetically to z spins in the adjacent layers. The exchange integrals are called $J'(>0)$ and $J(<0)$. The Zener carriers are allowed to hop both in the layer (with transfer integrals b') and also from one layer to the other (with transfer integrals b). The number of magnetic ions per unit volume is called N, and the number of Zener carriers Nx. We shall consider configurations in which all spins within each layer remain parallel, but where the angle between magnetizations of successive layers takes a prescribed value θ. We determine Θ_0 by minimizing the sum of exchange and double exchange energies. The exchange contribution is

$$E_{ex}=-Nz'J'S^2+Nz|J|S^2\cos\Theta_0. \tag{4}$$

To obtain the double exchange contribution we first compute the energy E_k of a Zener carrier of wave vector k. The amplitude of the carrier wave function is $\alpha_i=e^{i\mathbf{k}\cdot\mathbf{R}_i}$ and Eqs. (1) and (3) give us

$$E_k=\sum t_{ij}e^{i\mathbf{k}\cdot(\mathbf{R}_j-\mathbf{R}_i)} \tag{5}$$

$$=-b'\gamma_k'-b\gamma_k\cos(\Theta_0/2) \tag{6}$$

where $\gamma_k'=\sum_j' e^{i\mathbf{k}\cdot(\mathbf{R}_j-\mathbf{R}_i)}$ and $\gamma_k=\sum_j e^{i\mathbf{k}\cdot(\mathbf{R}_j-\mathbf{R}_i)}$ are sums extended to the nearest neighbors of site (i) which are respectively in the same layer or in different ones (note that $\gamma_0'=z'$, $\gamma_0=z$). As explained in the introduction, we are only interested in the bottom of the energy band defined by (6) because we restrict ourselves to a small carrier concentration ($x\ll1$). The minimum of (6) depends on the geometrical configuration of the magnetic lattice, and on the sign of b and b'. We shall simplify the discussion by assuming (arbitrarily) that b and b' are positive. Then

$$E_m=-\gamma_0'b'-\gamma_0 b\cos(\Theta_0/2). \tag{7}$$

Other signs for b and b' would lead to the same physical results but sometimes require a more complicated notation (when the band is not symmetrical). For simple layer configurations like the one shown on Fig. (2a), Eq. (7) is always valid provided we replace b and b' by their absolute value. The carriers, being few in number, occupy only energy levels close to E_m and the total double exchange energy is

$$E_d=NxE_m. \tag{8}$$

Minimizing the sum of (4) and (8) with respect to Θ_0 we get

$$\cos(\Theta_0/2)=bx/4|J|S^2 \tag{9}$$

$$E=E_{ex}+E_d=N[-z'J'S^2-xz'b'-z|J|S^2-(z/8)b^2x^2/|J|S^2]. \tag{10}$$

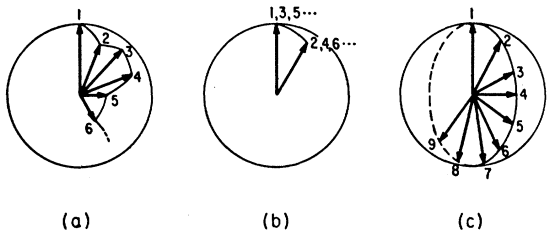

FIG. 1. Allowed configurations for the magnetizations $\mathbf{I}_1$, $\mathbf{I}_2$, $\mathbf{I}_3$, $\cdots$, $\mathbf{I}_n$, $\cdots$ corresponding to successive layers. The angle between $\mathbf{I}_n$ and $\mathbf{I}_{n+1}$ is equal to Θ_0. (a) disordered; (b) two sublattice system; (c) helical arrangement. (a), (b), and (c) are degenerate from the standpoint of nearest neighbor exchange and double exchange. External fields, anisotropy energies, or small ferromagnetic couplings between next nearest layers favor configuration (b). Antiferromagnetic coupling between next nearest layers favors (c).

For $x<4|J|S^2/b$ Eq. (9) defines an angle Θ_0 between 0 and π, and the magnetizations in the successive layers point in different directions.

All arrangements which satisfy Eq. (9) are degenerate. There is a large number of them, because, when we go from layer n to layer $n+1$ the magnetic moment I_{n+1} of layer $(n+1)$ is allowed to take any orientation on a cone (of some angle θ) around I_n. A typical arrangement is shown on Fig. 1(a). The degeneracy is removed by energy terms not included in our model, of which the most important are probably magnetocrystalline energies. For general values of θ, the simple two-sublattice ordering of Fig. 1(b) is then stabilized. For some special values of θ (e.g., $\theta=2\pi/n$, where n is a small integer) a helical arrangement as shown on Fig. 1(c) might still be degenerate with the two-sublattice arrangement. However, this is an exceptional situation, and even then a small magnetic field is enough to restore the two-sublattice ordering, where a nonzero spontaneous moment is present. It is probably worthwhile at this stage to point out the difference between the ordering of Fig. 3(c) and the helical spin arrangements considered by Villain,[6] Yoshimori and Kaplan[7] in materials with pure exchange forces. The latter arrangements are nondegenerate (apart from trivial degeneracies due to crystal symmetries) and can be destroyed only by magnetic fields of the order of the exchange field. In our case, on the other hand, all the orderings shown in Fig. 1 are degenerate, and only a few of the, such as 1(b), are not destroyed by application of an external field. In the following we shall restrict our attention to two-sublattice systems of type 1(b). The general case will be considered briefly in Sec. V. We now derive a few important properties of our spin assembly at $T=0$.

(1) The spontaneous magnetization of the two sublattice arrangement is

$$M=I\cos(\Theta_0/2) \tag{11}$$

[6] J. Villain, J. Phys. Chem. Solids **11**, 303 (1959).
[7] A. Yoshimori, J. Phys. Soc. (Japan) **14**, 807 (1959); T. H. Kaplan, Phys. Rev. **116**, 888 (1959).

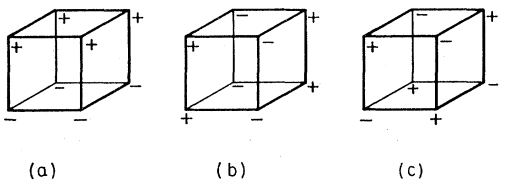

FIG. 2. Examples of "layer" antiferromagnet (2a), "chain" antiferromagnet (2b), and "alternating" antiferromagnet (2c) in a simple cubic lattice. The (2a) structure is observed in $LaMnO_3$, the (2c) structure in $CaMnO_3$.[2]

where $I/2$ is the magnetization of one sublattice. By making use of Eq. (9) this becomes

$$M/I = bx/4|J|S^2. \tag{12}$$

The ferromagnetic moment is accordingly proportional to x (at low x).

(2) There is a nonzero susceptibility in high fields, due to a field induced change in angle between sublattices. This susceptibility is isotropic, because in high fields all magnetocrystalline terms are expected to be negligible. The spin system rotates to set its moment parallel to the field. The Zeeman energy is

$$E_Z = -HI\cos(\Theta/2), \tag{13}$$

and the moment is always given by (11), but with an angle Θ between sublattices different from Θ_0. We derive Θ by taking the minimum of the sum (4), (7), and (13):

$$\cos(\Theta/2) = (bx/4|J|S^2) + HI/4|J|NS^2\gamma_0. \tag{14}$$

The susceptibility is then

$$\chi = I^2/4|J|\gamma_0 S^2 N. \tag{15}$$

Apart from possible small corrections in I, it is identical to the transverse susceptibility of the pure material. It could be measured by the same experimental techniques which have been applied to triangular spin arrangements in spinels.[8] In the manganite series such a lack of saturation in high fields has been qualitatively observed.[2]

(3) The magnetic scattering of neutrons shows an unusual pattern. Let us call $\mathbf{\mu}_1$ and $\mathbf{\mu}_2$ respectively the moments carried by one spin on each sublattice, and put $\mu = \mu_1 = \mu_2$. The scattering intensity if proportional to the square of: $\mathbf{u} = (1/k)\mathbf{k} \times (\mathbf{\mu}_1 \pm \mathbf{\mu}_2)$ where $\mathbf{k}$ is the scattering vector,[9] and the + or − sign correspond respectively to "lattice" reflections (L) (where both sublattices are in phase) and to "superlattice" reflections (S) (where they are opposite in phase). *Both types of reflections are simultaneously observed* in general. For instance, if $\mathbf{k}$ is perpendicular to the plane $(\mathbf{\mu}_1\mathbf{\mu}_2)$ of the spins the (L) and (S) intensities are respectively proportional to $\cos^2(\Theta_0/2)$ and $\sin^2(\Theta_0/2)$ where Θ_0 is defined by (9). We see that neutron diffraction measures Θ_0 directly. Using the notation of Wollan and Koehler[2] we may write

$$\mu_{\text{ferro}}^2 = \mu^2\cos^2(\Theta_0/2), \tag{16a}$$

$$\mu_{\text{antif}}^2 = \mu^2\sin^2(\Theta_0/2). \tag{16b}$$

We now apply the above considerations to the experimental data on the manganites[2] for low Mn^{4+} content. Pure $LaMnO_3$ is indeed a layer antiferromagnet, as shown on Fig. 2. For the mixed compounds, we derive from (16a) and (16b) two sets of values for $\cos(\Theta_0/2)$ as a function of x. These values are plotted on Fig. 3. It may be seen that they coincide rather well, and that the linear relation (9), with all effects of higher order in x neglected, accounts reasonably for the data. From the slope of this plot we infer that $b/|J|S^2 \sim 16$. (Unfortunately we have no information on the interlayer exchange constant $|J|$ in $LaMnO_3$.) This figure shows incidentally that the carrier band width is indeed large when compared with the exchange energies in the pure material, as mentioned in the introduction.

We shall now discuss briefly the effect of an applied magnetic field on the neutron lines. If this field is applied parallel to the scattering vector $\mathbf{k}$, and if it is strong enough to overcome all anisotropy forces, the ferromagnetic reflections are extinguished. On the other hand, if the anisotropy fields are comparable in strength to the applied field, a very complicated situation is obtained, and the (L) lines are not completely extinguished. This appears to be the case in the mixed manganites with low Mn^{4+} content.

We observe incidentally that if helical arrangements were stabilized by some auxiliary coupling (such as a small antiferromagnetic exchange between next nearest layers) they would give rise to another class of neutron lines, which cannot in general be indexed in any multiple of the unit cell.[7]

(4) Another interesting question is related to possible nuclear resonance experiments on nonmagnetic ions belonging to the structure. Assume for instance that the magnetic atoms within different layers are separated

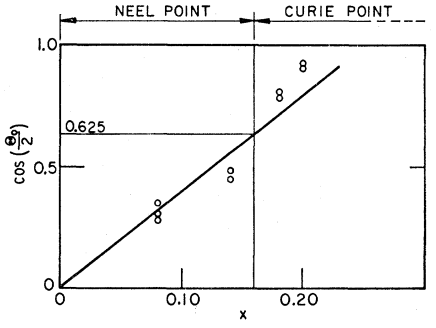

FIG. 3. Determination of the angle Θ_0 between sublattices in the mixed manganites $La_{1-x}Ca_xMnO_3$ with low Mn^{4+} content. The experimental points are deduced from measurements of "ferromagnetic" and "antiferromagnetic" neutron line intensities by Wollan and Koehler.[2] The straight line corresponds to Eq. (9) with $b/|J|S^2 = 16$.

[8] I. S. Jacobs, J. Phys. Chem. Solids **11**, 1 (1959).
[9] O. Halpern and M. H. Johnson, Phys. Rev. **55**, 898 (1939).

by fluorine ions, and that the environment of each fluorine contains an equal number of spins from sublattices 1 and 2. Then, in the pure material, we expect that the hyperfine fields acting on the F^{19} nucleus due to both sublattices will cancel exactly. In the mixed compounds however, they will not, and there will be a shift in the resonance, proportional to $\cos(\theta/2)$. One expects two types of nuclear relaxation due to coupling with (a) the carriers and (b) the spin waves. From the spin lattice times measured both in antiferromagnetic insulators[10] and in ferromagnetic metals,[11] we infer that relaxation effects should not prevent observation of the line. Unfortunately, there are inhomogeneities in the hyperfine field due to local spin distortions not included in the present model (see Sec. IV). This inhomogeneous broadening is expected to be large, and the experiment does not seem feasible.

This section has been restricted to calculations on "layer" antiferromagnets. We would like to mention that there is another class of antiferromagnetic materials where carrier motion is allowed in the unperturbed structure, namely the "chain" structure, an example of which is shown on Fig. 2(b). Considerations very similar to the above may be applied there. The number of allowed canted arrangements which are degenerate with respect to exchange and double exchange is increased: the only requirement is again that the angle between the magnetizations carried by neighboring chains is equal to some fixed value Θ_0. This can be accomplished in many ways and configurations with more than two sublattices may have to be considered here even when magnetocrystalline forces are present.

III. MAGNETIC BEHAVIOR AT FINITE TEMPERATURES

The statistical properties of our spin assembly at finite temperatures may be approached by a study of elementary excitations (spin waves) or by some extension of the molecular field concept. Both techniques are much increased in complexity when double exchange carriers are present. The most interesting property finally to be displayed is the existence of a first transition point when the canted arrangement collapses, the system becoming ferro- or antiferromagnetic at higher temperatures. This property is beyond the scope of spin-wave analysis, and we accordingly concentrate here on the more useful molecular field description. (The low-frequency spin-wave spectrum is considered in Appendix 1.) A first step is to derive the energy of carriers at the bottom of the band where the ionic spins are not completely ordered. We get an approximate value for this energy by taking as a variational wave function in Eq. (2) the very simplest one where all α_i's are equal. (This is the exact eigenfunction for all ordered states with our choice of sign for the transfer integrals.) We obtain

$$E_m = -\sum_j b_{ij}\langle\cos(\theta_{ij}/2)\rangle$$

where the $\langle\ \rangle$ symbol represents a thermal average on the possible states of the ionic spins. We may rewrite the preceding equation for our layer antiferromagnet in the form

$$E_m = -\gamma_0 b\langle\cos(\theta/2)\rangle - \gamma_0' b'\langle\cos(\theta'/2)\rangle \qquad (17)$$

where θ' and θ are the angles between any ionic spin and its neighbors respectively in and out of the layer. We now make use of the molecular field approximation in the following way: we neglect all correlations between different ionic spins, and assume for each of them a statistical distribution corresponding to a molecular field.

$$w_n(\mathbf{S}) = (1/\nu)\exp(-\lambda_n\cdot\mathbf{S}/S). \qquad (18)$$

The index n specifies the sublattice to which $\mathbf{S}$ belongs ($n=1$ or 2); λ_n is proportional to the molecular field acting on sublattice (n). The two molecular fields are equal in length ($\lambda_1=\lambda_2=\lambda$) and the angle between them is Θ. The normalization constant ν is:

$$\nu = \int_{-1}^{1} du e^{-\lambda u} = 2(\sinh\lambda)/\lambda. \qquad (19)$$

The relative amount of saturation of each sublattice is:

$$m = \frac{1}{\nu}\int_{-1}^{1} du u e^{-\lambda u} = -(1/\lambda) + \operatorname{ctanh}\lambda. \qquad (20)$$

Our aim is to insert the assumed distribution function (18) into a variational principle for the free energy. We first derive the entropy term:

$$-TS = Nk_BT\int_{-1}^{1} w(x)\ln w(x)dx = Nk_BT(\lambda m - \ln\nu). \qquad (21)$$

The calculation of the energy term is somewhat more complicated. Consider for instance the first term of (17), which corresponds to double exchange between sublattices. Let us write

$$\cos(\theta/2) = \sum_{l=0}^{l=\infty} A_l P_l(\cos\theta). \qquad (22)$$

The coefficients A_l can be obtained from the generating function of the P_l's (see Appendix 2). They are given by

$$A_l = (-)^{l+1}\frac{2}{(2l-1)(2l+3)}. \qquad (23)$$

[10] R. G. Shulman and V. Jaccarino, Phys. Rev. **108**, 1219 (1957).
[11] A. C. Gossard and A. M. Portis, Phys. Rev. Letters **3**, 164 (1959).

We then express $P_l(\cos\theta)$ in terms of the polar angles of the two spins S_1, S_2 which serve to define the angle θ. The average orientations of S_1 and S_2 are not parallel; since they belong to different sublattices, the angle between them is Θ. It is convenient to refer the polar angles $(\theta_1\varphi_1)$ of $\mathbf{S}_1$ to a polar axis parallel to $\mathfrak{A}_1$ and $(\theta_2\varphi_2)$ to an axis parallel to $\mathfrak{A}_2$. With the usual notation for spherical harmonics $Y_{lm}(\theta\varphi)$ and Wigner rotation coefficients D^l, we get:

$$P_l(\cos\theta)=N_l\sum_{mm'}Y_{lm}(\theta_1\varphi_1)Y_{lm'}{}^*(\theta_2\varphi_2)D_{mm'}{}^l(0,\Theta,0). \tag{24}$$

The N_l are normalization factors. Let us take the thermal average of (24) with independent statistical distributions w_1, w_2 as defined in (18). The only non-zero term corresponds to $m=m'=0$. $D_{00}{}^l(0,\Theta,0)$ is simply a Legendre polynomial, and the final result is

$$\langle P_l(\cos\theta)\rangle=\langle P_l(\cos\theta_1)\rangle\langle P_l(\cos\theta_2)\rangle P_l(\cos\Theta). \tag{25}$$

Furthermore

$$\langle P_l(\cos\theta_1)\rangle=\frac{1}{\nu}\int_{-1}^{1}e^{-\lambda u}P_l(u)du$$
$$=(2/\nu)i^l j_l(-i\lambda) \tag{26}$$

where j_l is the usual spherical Bessel function, taken here for an imaginary argument. Collecting the results of Eq. (22) to Eq. (26) we obtain

$$\langle\cos(\theta/2)\rangle=-\frac{2}{j_0{}^2(-i\lambda)}\sum_{l=0}^{\infty}\frac{j_l{}^2(-i\lambda)P_l(\cos\Theta)}{(2l-1)(2l+3)}. \tag{27}$$

In a similar way, if we deal with the angle θ' of two neighboring spins belonging to the same sublattice, we obtain

$$\langle\cos(\theta'/2)\rangle=-\frac{2}{j_0{}^2(-i\lambda)}\sum_{l=0}^{\infty}\frac{j_l{}^2(-i\lambda)}{(2l-1)(2l+3)}. \tag{28}$$

We insert (27) and (28) in (17), and multiply by the number Nx of carriers to obtain the total double exchange energy

$$E_D=\frac{2Nxz}{j_0{}^2(-i\lambda)}\sum_{l=0}^{\infty}\frac{j_l{}^2(-i\lambda)}{(2l-1)(2l+3)}$$
$$\times[\gamma_0 bP_l(\cos\Theta)+\gamma_0'b']. \tag{29}$$

Since λ is related to the sublattice magnetization m by Eq. (20), we may consider (29) as expressing the double exchange energy in terms of the macroscopic parameters m and Θ. We will have to add the usual exchange energy

$$E_{ex}=-Nm^2(z'J'+zJ\cos\Theta). \tag{30}$$

The free energy F is the sum

$$F=-TS+E_D+E_{ex}. \tag{31}$$

This has to be a minimum with respect to λ (or m) and with respect to Θ. Let us first carry out the variation with respect to $\cos\Theta$. We obtain

$$m^2+\frac{2\xi}{j_0{}^2(-i\lambda)}\sum_l\frac{j_l{}^2(-i\lambda)}{(2l-1)(2l+3)}\frac{dP_l(v)}{dv}=0 \tag{32}$$

where $\xi=bx/|J|S^2$ and $v=\cos\Theta$. For each λ (31) is an implicit equation for v. For large λ (low temperatures) the solution v_m is such that $-1<v_m<1$: the spin arrangement is canted. For small λ (higher temperatures) v_m is outside the interval $(-1, 1)$: the equilibrium configuration is ferromagnetic $(v_m>1)$ or antiferromagnetic $(v_m<-1)$. The critical value of λ (or m) is obtained by setting $v=\pm1$ in Eq. (32), and observing that

$$\left(\frac{dP_l(v)}{dv}\right)_{v=1}=\tfrac{1}{2}l(l+1)$$
$$\left(\frac{dP_l(v)}{dv}\right)_{v=-1}=(-)^{l+1}\tfrac{1}{2}l(l+1). \tag{33}$$

The resulting equations for the critical λ's may be written in the form

$$\frac{1}{\xi}=\frac{1}{j_1{}^2(-i\lambda)}\sum_{l=1}^{\infty}\frac{l(l+1)}{(2l-1)(2l+3)}j_l{}^2(-i\lambda)$$

(canted to ferro) (34a)

$$\frac{1}{\xi}=-\frac{1}{j_1{}^2(-i\lambda)}\sum_{l=1}^{\infty}(-)^l\frac{l(l+1)}{(2l-1)(2l+3)}j_l{}^2(-i\lambda)$$

(canted to antiferro). (34b)

For finite λ the convergence of these series is good. λ and m are related by Eq. (20), and the best graphical representation of Eq. (34) is in fact obtained by plotting m^2 as a function of ξ (Fig. 4). We see immediately from this plot that for small m the arrangement is never canted (except for the special value $\xi=2.5$.) The upper transition point always corresponds to a colinear configuration for the magnetizations of both sublattices. By lowering the temperature, however, we increase m and finally intersect the critical curve at a well-defined temperature T_1 which we refer to as the second critical point. It may be shown that m and Θ are both continuous functions of temperature at $T=T_1$. A complete study of the thermal behavior is complicated by the large number of independent parameters which come into play (J,J',b,b'). This is why Eq. (34), which involves only one parameter (ξ), is of particular interest.

We now consider the dependence of the free energy (31) on m in the "colinear" range (above T_1), and more specifically the limit of small m, which corresponds to the upper Curie point. Equation (31) may be expanded

in the following form:

$$F=F_0+F_2m^2+F_4m^4+\cdots \tag{35}$$

where

$$(1/N)F_2=\tfrac{3}{2}k_BT-S^2(z'J'+zJv)-(2x/5)(z'b'+vzb). \tag{36}$$

We know from the preceding argument that only the parallel ($v=1$) and antiparallel ($v=-1$) cases have to be considered, in which case F_4 takes the simple form

$$(1/N)F_4=(6x/7\times 25)(z'b'+zb)+(9/20)k_BT. \tag{37}$$

We now write that (35) is a minimum and obtain

$$m^2=-(F_2/2F_4). \tag{38}$$

The upper transition point corresponds to $F_2=0$. It is given by the greater of the two quantities quoted in the following:

$$T_C=(2/3k_B)[(zJ+z'J')S^2+(2x/5)(z'b'+zb)] \quad \text{(Curie point)} \tag{39a}$$

$$T_N=(2/3k_B)[(-zJ+z'J')S^2+(2x/5)(z'b'-zb)] \quad \text{(Néel point)}. \tag{39b}$$

(Remember that for the cases in which we are interested J is negative and J' positive.) We emphasize the fact that only two transition points are observed in all cases (T_1 and T_C or T_1 and T_N). Another interesting quantity is the paramagnetic Curie point T_P defined through the asymptotic form of the paramagnetic susceptibility $\chi=C/(T-T_P)$. When the carrier band width is small compared to k_BT there is no contribution to T_P from the double exchange effect, as emphasized by Anderson and Hasegawa.[4] On the other hand, when k_BT remains small compared with the band width, as it probably

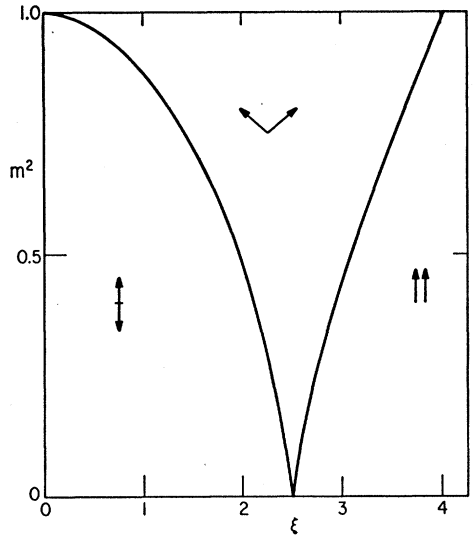

FIG. 4. Square of the relative saturation $m_{T1}=M_{T1}/M_0$ of each sublattice at the lower transition point T_1, as a function of $\xi=bx/|J|S^2$.

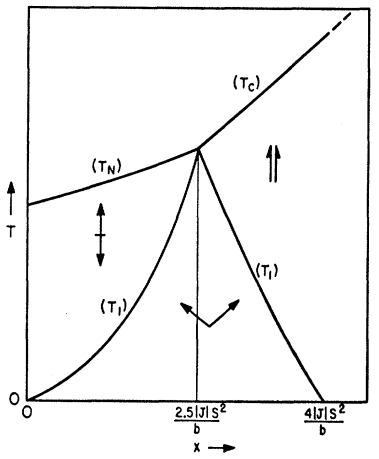

FIG. 5. Typical "magnetic phase diagram" for a layer antiferromagnet. Theoretical values of T_1, T_c, and T_N are given in the text.

does in practice, our approximation scheme remains valid. If we retain the same simple form of variational wave function to obtain the carrier ground-state energy, we can show by the Van Vleck trace method that

$$k_BT_P=\tfrac{2}{3}S^2\textstyle\sum_j J_{0j}+(4x/15)\sum_j b_{0j} \tag{40}$$

so that T_P and T_C coincide within the molecular approximation, as in the more familiar case of pure exchange. It is not possible to derive simple expressions for the lower transition point T_1, except in the limiting case where ξ is not very different from 2.5. It is then easy to see from Fig. 4 that the transition (T_1) occurs for small values of m, so that the expansion (35) for the free energy may be used on the whole temperature interval between the two transition points. In this range of ξ values Eqs. (34a) and (34b) for $[m]_{T1}$ take the simple form

$$[m^2]_{T1}=\frac{175}{18}\left|\frac{1}{\xi}-\frac{2}{5}\right|. \tag{41}$$

By eliminating m^2 between (41) and (38) we get

$$T_1=T_0-\frac{2}{3k_B}\left|\frac{1}{\xi}-\frac{2}{5}\right|\left[\frac{2x}{3}(zb+z'b')+\frac{35}{4}k_BT_0\right]\times\left|\frac{1}{\xi}-\frac{2}{5}\right|\ll 1 \tag{42}$$

where T_0 is the upper transition point as defined by (39). Figure 5 shows qualitatively the stability domains of the different spin configurations when both the temperature T and the parameter ξ (proportional to x) are raised. The angle Θ_0 between sublattices in the ground state is given by (9). When Θ_0 is larger than 103° ($\xi<2.5$) the canted arrangement becomes antiferromagnetic by raising the temperature above T_1. When Θ_0 is smaller than 103° ($4>\xi>2.5$) it becomes ferromagnetic.

We close this section by a brief discussion of the

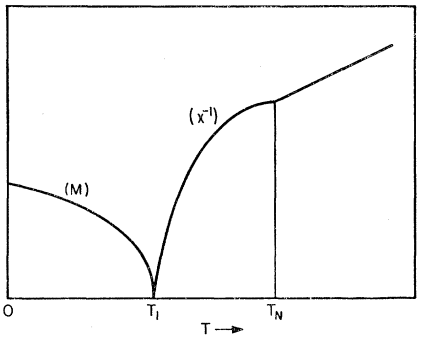

FIG. 6. Typical plot of inverse susceptibility and spontaneous magnetization when $\xi<2.5$ (magnetocrystalline energies are neglected).

physical anomalies which are expected of the lower transition point T_1.

(1) The behavior of the susceptibility χ is remarkable when the upper transition point is antiferromagnetic. By decreasing T we first observe the usual discontinuity in slope at T_N. Then χ increases and becomes infinite at T_1. The qualitative behavior of $1/\chi$ is shown on Fig. 6. Experimental results very similar in their general appearance to the graph of Fig. 6 have been obtained in antiferromagnetic CrSb doped with a small amount of MnSb.[12] The pure compound CrSb is known to be of the antiferromagnetic layer type.[13] It may be that electron transfer is allowed between chromium and manganese atoms, in which case our model could be applied.

(2) Below T_1 both ferromagnetic and antiferromagnetic neutron lines occur simultaneously. Above T_1 only one type is observed. A phenomenon of this type has been indeed quoted by Wollan and Koehler for some mixed manganite samples.[2]

(3) The specific heat shows a (small) discontinuity at $T=T_1$.

(4) The electrical conductivity is favored by interlayer transfer. We accordingly expect a slight discontinuity in slope at $T=T_1$. The sign of this discontinuity will depend on the type of order above T_1. However, our oversimplified model is not applicable to this problem, and we are not able to make more detailed predictions as regards this point.

IV. LOCAL SPIN DISTORTIONS

1. Bound States

The simple model of Secs. II and III did not take into account any possible bound states of the carriers. Such bound states may in fact occur, especially when the amount of impurities is very small. For instance, each Ca^{2+} substituted for La^{3+} in $LaMnO_3$ acts as an effective charge $-e$ and is able to accept one carrier (a hole) in a localized orbit. We intend to show that the over-all effects of an assembly of such centers on the ionic spin system are similar to those of the free carriers considered in the preceding Section. We consider in particular the extreme case where the wave functions relative to different impurity centers do not overlap (very small x). In analogy with the known properties of color centers in alkali halides, we expect the wave functions to be of rather small extension; in the above example, the hole will be shared by the eight manganese atoms surrounding the impurity, as shown on Fig. 7.

We first consider a single impurity center in an unperturbed antiferromagnetic matrix, and restrict ourselves to the following simple example: the pure material is an "alternating" ferromagnet of one simple cubic [see Fig. 2(c)] or bcc structure, with exchange integral J coupling each spin to its z neighbors. The Zener electron (or hole) is strongly bound and can only occupy *two* neighboring sites (1) and (2). The transfer integral is $t_{12}=b\cos(\theta_{12}/2)$ as before, and the propagation equations which replace (2) are

$$\begin{aligned}(E-U)\alpha_1&=b\cos(\theta_{12}/2)\alpha_2\\(E-U)\alpha_2&=b\cos(\theta_{12}/2)\alpha_1\end{aligned}\tag{43}$$

where U is the binding energy. (Note that the value of b may be modified by the attractive potential.) The ground state corresponds to

$$E_D=U-b\cos(\theta_{12}/2).\tag{44}$$

This is the analog, for a localized state, of Eq. (7) which applied to an extended state. In both cases, a small departure of θ_{12} from π decreases the double exchange energy in first order and increases the exchange energies only in second order, so that a canted arrangement will be stable. Here, however, the final configuration corresponds to a local distortion of the spin system, and is accordingly more difficult to compute. We shall first derive the amount of canting by a simple "rigid field approximation" (RFA) where all ionic spins other than $\mathbf{S}_1$ and $\mathbf{S}_2$ are assumed to retain their original orienta-

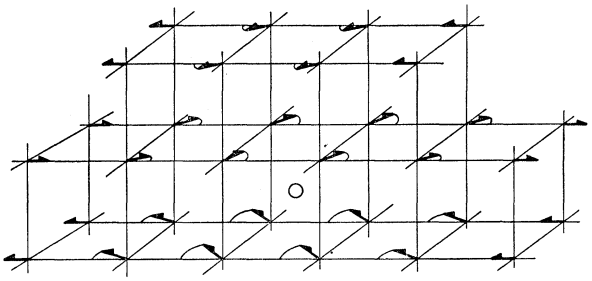

FIG. 7. Local spin distortion in $LaMnO_3$. The bound hole is localized on eight manganese atoms (black circles) around the impurity center Ca^{2+} (open circle). All ionic spins remain in one plane [here taken to be (001)]. Deflections are maximum close to the impurity center, but they decrease only slowly with distance.

[12] T. Hirone, S. Maeda, and I. Tsubokawa, J. Phys. Soc. (Japan) **11**, 1083 (1956); E. W. Gorter and F. K. Lotgering, J. Phys. Chem. Solids **3**, 238 (1957).

[13] A. I. Snow, Revs. Modern Phys. **25**, 127 (1953).

tion. $\mathbf{S}_1$ and $\mathbf{S}_2$ have opposite deflections ϵ and $-\epsilon$ and $\theta_{12}=\pi-2\epsilon$. The increase in exchange energy is

$$E_{ex}=2|J|S^2[2(z-1)(1-\cos\epsilon)+1-\cos 2\epsilon]. \quad (45)$$

The minimum of the sum of (44) and (45) corresponds to

$$-b\cos\epsilon+2|J|S^2[2(z-1)+4\cos\epsilon]\sin\epsilon=0. \quad (46)$$

This always gives a solution ϵ, with the limiting forms

$$\begin{aligned}\epsilon&=\frac{b}{4|J|S^2(z+1)}; \quad (b/z|J|S^2\ll 1)\\ \epsilon&=\frac{\pi}{2}-\frac{4|J|S^2(z-1)}{b}; \quad (b/z|J|S^2\gg 1).\end{aligned} \quad (47)$$

A bound Zener electron *always* gives rise to a local distortion of the spin system. This is to be contrasted with the effects which are obtained with pure exchange, when some adequate substitution simply changes the sign of one exchange integral, between (1) and (2). In the latter case there is also a strongly inhomogeneous constraint applied to the spin system. However, this results in a local spin distortion only if the new (ferromagnetic) exchange integral exceeds a well-defined threshold value ($J_{new}>\frac{1}{2}(z-1)|J|$ in RFA, and $J_{new}>\frac{1}{2}(z-2)|J|$ by an exact calculation).

We have proved that in the vicinity of each impurity center there is an unbalanced magnetic moment due to the special effects of double exchange. There is however one feature which is deliberately neglected in the RFA: a local deflection of spins (1) and (2) is always accompanied by smaller distortions on the neighboring sites, the amplitude of which decreases only slowly with distance. These "wings" may be studied with good accuracy by making use of Green's function techniques, an example of which is given in Appendix 3. If we now consider not only one impurity but a dilute assembly of these, the "wings" result in a coupling of the unbalanced moments carried by the different impurity centers. At low temperatures it is energetically favorable for these moments to line up, thus reducing the spin distortions in the matrix. As a result we expect to observe a nonzero spontaneous moment, increasing linearly with x, and the over-all magnetic behavior is very similar to what we found in Sec. II by discussing free carriers. We also expect the "interlocking" between different centers to preserve this ordered state up to some critical temperature T_1, above which the unbalanced moments exhibit a paramagnetic behavior. Here again, the conclusions of the "free carrier model" and of the "color center model" are not very different.

We now mention briefly some phenomena for which both models do *not* lead to the same predictions for very dilute impurity systems. These are: (1) optical absorptions; (2) electrical conductivities; (3) nuclear resonance at anion sites; (4) neutron diffraction. The nuclear resonance lines are widely broadened, because the long-range part of the spin distortion due to each individual impurity center is responsible for inhomogeneous hyperfine fields. Consequently this type of experiment seems difficult to carry out. Neutron diffraction studies, on the other hand, could give some very interesting information on local spin distortions. This is discussed in Appendix 3, the main conclusions of which may be summarized as follows. (a) The distortions lead to diffuse peaks around the superlattice line. Superlattice lines for which the scattering vector is parallel to the spin direction in the pure material are extinguished and consequently most favorable. (b) There is always a parasitic spin wave scattering even at low temperatures (because of the strong zero point motion effects in antiferromagnets). (c) However, spin wave emission is an inelastic process while scattering by static distortions is strictly elastic. As a result, by a suitable geometrical arrangement one can make the spin wave scattering very diffuse so that it will be automatically subtracted with the background. The final requirement is that the neutron spectrometer should be able to analyze an angular distribution corresponding to a diffuse peak whose integrated intensity is roughly x times smaller than the intensity of a typical magnetic line of the unperturbed structure. A typical value of x (small enough to reduce overlap between separate distortions) is 0.1, so that this figure is not prohibitive.

2. Self-Trapped Carriers

Sections II and III applied the "free carrier" model to layer and chain antiferromagnets, where the carriers are always allowed to move within each chain or layer. The "alternating" antiferromagnetic structures (where all neighbors of a + spin are − spins) are somewhat different; in the unperturbed structure the carriers are not allowed to move; it is then more favorable for each individual carrier to build up a *local* distortion of the spin lattice in which it becomes "self-trapped." The resulting centers are able to move only slowly, and their physical properties are modified. In practice, we are not very much concerned in effects such as a change in effective mass, because the slow carriers will always fall into bound states. We are mainly interested in the shape of the local distortions and in interactions between them.

We first show that self-trapping will indeed occur. The argument will be written down for a simple cubic- or body-centered cubic "alternating" antiferromagnet, each ionic spin having z equivalent neighbors, with exchange couplings $2JS^2\cos\theta_{ij}$, transfer integrals $b\cos(\theta_{ij}/2)$, and carrier concentration x defined as before. Let us first compute the gain in energy for a uniform canting of both sublattices in the free carrier model, as in Sec. II. We obtain

$$E_{free}=-\tfrac{1}{8}Nzb^2x^2/|J|S^2. \quad (48)$$

It is convenient to introduce the paramagnetic Néel point $T_N=[(2|J|S^2z)/3k_B]$ of the pure material, and the dimensionless ratio $\eta=b/k_BT_N$, so that Eq. (48) becomes:

$$E_{\text{free}}/k_BT_N=-(N/12)z^2\eta^2x^2. \tag{49}$$

We now consider another possible configuration, with noninteracting localized states, and compute the corresponding energy by making use of a variational principle. We assume that the carrier to be considered is trapped on some magnetic site (which we call 0 for instance) with an amplitude α_0, but we also allow it to have a nonzero amplitude α_1 on the z neighboring spins. As far as the ionic spins are concerned, we assume that they all retain the same orientation which they had in the pure material, except for $\mathbf{S}_0$, which is allowed to make an arbitrary angle θ with the common direction of the z neighboring spins. The exchange energy, counted from the initial configuration ($\theta=\pi$) is

$$E_{\text{ex}}=2|J|S^2z(1+\cos\theta). \tag{50}$$

The wave equation for the trapped carrier takes the restricted form

$$\begin{aligned} E\alpha_0&=zb\cos(\theta/2)\alpha_1 \\ E\alpha_1&=b\cos(\theta/2)\alpha_0 \end{aligned} \tag{51}$$

and the ground-state carrier energy is

$$E_D=-b\sqrt{z}\cos(\theta/2). \tag{52}$$

By taking the minimum of $E_{\text{ex}}+E_D$ we obtain an overestimate of the energy per trapped carrier E_1

$$E_1/k_BT_N=-(z/24)\eta^2 \quad \text{if} \quad \eta<12/\sqrt{z} \tag{53a}$$

$$=6-\sqrt{z}\eta \qquad \eta>12/\sqrt{z}. \tag{53b}$$

Actually this estimate is not accurate for large couplings ($\eta\gg1$) where the "radius" of the trapped carrier exceeds one interatomic distance. Equation (53) is sufficient for our purposes, however, and shows that E_1 is negative. The total energy of the trapped carriers NxE_1 is proportional to x, while the energy (49) corresponding to uniform canting goes like x^2. At low x the self-trapped configuration is always more stable. The following remarks should be made.

(1) Equation (49) represents the average effect of an attractive interaction between carriers via the ionic spins; each carrier tends to cant the antiferromagnetic lattice and decreases the energy of all other carriers at the bottom of the band. This explains the x^2 dependence of (48).

(2) In layer antiferromagnets, the energy of the free carrier model contains a negative term, due to intralayer motion, and proportional to the number of carriers x; self-trapped states are much less favored in such structures. (Of course, in practice, we shall find bound states as explained earlier.) Another viewpoint, leading to the same result, is the following: in a layer or chain antiferromagnet spin distortions contribute only to a part of the band energy, and the coupling between carriers and ionic spins is moderately strong when compared with the unperturbed energy of the carriers. On the other hand, the coupling is very strong in an alternating antiferromagnet, since *all* the carrier energy is due to distortions of the spin arrangement.

The over-all effect of self-trapped carriers on magnetostatic properties is complex, and probably unobservable because of the existence of bound states. We shall restrict ourselves here to a few qualitative remarks, related to the behavior of the mixed manganites with *high* Mn^{4+} content. Pure $CaMnO_3$ is an alternating antiferromagnet (simple cubic). The mixtures of neighboring compositions are not conducting and do not show any ferromagnetic behavior. This has been interpreted by Goodenough[14] by means of a qualitative model which is somewhat related to self-trapping. He assumes that the extra electron reverses the spin $\mathbf{S}_0$ of the central site (θ going from π to 0) but leaves all other spins unaltered. This then results in a simple reduction of the sublattice magnetization, and does not bring in any noncompensated moment, since there is an equal number of trapped carriers on both sublattices. We are not quite satisfied with this explanation, for the following reason: from Eqs. (50) and (52) we may show that the actual configuration of $\mathbf{S}_0$ is canted ($0<\theta<\pi$) when $\eta<12z^{-\frac{1}{2}}$. For larger η's, our simple variational wave function yields a ground state which agrees with the Goodenough picture, but it is not a good approximation any more. In fact it is easy to see that for such values of η the whole configuration built up by $\mathbf{S}_0$ and its six nearest neighbors becomes canted with respect to the more distant spins. In all cases there is a noncompensated magnetic moment directed perpendicularly to the spin direction of the unperturbed structure. Furthermore, this moment is always accompanied by a long-range distortion of the spin lattice. Exactly like in the case of bound states, we expect these long-range distortions to couple ferromagnetically the moments due to different carriers, in contradiction with experiment. We do not believe that the discrepancy can be explained within our simple model.

V. CONCLUSIONS

The special form of the double exchange coupling is such that all antiferromagnetic (and also all ferrimagnetic) spin arrangements are distorted as soon as some Zener carriers are present. This is due to the fact that electron transfer lowers the energy by a term of first order in the distortion, while the initial exchange energy is increased only in second order. If the Zener carriers are free to move in the structure, the distortion will usually correspond to a uniform canting of the sublattices. If they are bound or nearly bound, the distortion is nonhomogeneous, but the average effects are similar to the above. In practice the second alternative

[14] J. B. Goodenough, Phys. Rev. **100**, 564 (1955).

is closer to the actual state of affairs. However the "free carrier model," corresponding to the first alternative, is expected to provide a good starting point in all cases, when one is only interested in the macroscopic magnetic properties of the system.

We now write down a short list of the physical quantities which may be used to determine the relevant exchange and transfer integrals in a given "layer" antiferromagnet. These are: (1) the paramagnetic Curie point, the Néel point, and the low-temperature susceptibility of the pure material (from which one can extract J and J'). (2) The spontaneous moment at $T=0$ of the mixed materials (from which we get the ratio $b/|J|$ as shown by Eq. (11). This moment may be obtained both by neutron diffraction or by magnetostatic measurements (the latter being clear cut only if the moment is obtained by an extrapolation to low fields of the high field B-H curve, as has been done by Jacobs[8] for triangular spin arrangements in spinels). (3) The paramagnetic Curie point and the two transition points of the mixed compounds, as given by (39) and (40). Location of the transition points is achieved with the best accuracy by using specific heats and electrical conductivities. The numbers derived from low-temperature data are of course the most reliable, because they do not make use of the very naive approximations of Sec. III as regards the carrier energy levels and the statistical behavior. The assumption that the carrier bandwidth is large when compared to k_BT should also be checked, and could eventually be improved.

In Sec. II we emphasized the fact that many degenerate canted configurations are always allowed in the presence of double exchange as illustrated by Fig. 1. Only the simplest (two sublattice) types were considered and the question may be raised whether this is a serious restriction or not. We now present some remarks related with the more general situation. (a) In spite of the degeneracy one and only one arrangement is stable at each temperature. This may be seen in the following way: if we go to a partially disordered state as shown in Fig. 1(a) we lower the free energy by an entropy term proportional to the number of layers ($\sim N^{\frac{1}{3}}$) or of chains ($\sim N^{\frac{2}{3}}$). On the other hand, the small magnetocrystalline or next nearest neighbor exchange terms are modified by an amount proportional to N; their contribution always dominates, and the only observable arrangements are those for which it is a minimum. (b) Of course, even these small energy terms do not remove the degeneracy between arrangements which can be deduced from one another by a symmetry operation of the lattice group. The crystal may accordingly break up into domains, and the domain wall energy may be extremely small in some cases. As an example think of two helical arrangements corresponding to Fig. 1(c), one right-handed, the other left-handed, with a sharp boundary parallel to the plane of the layers; the wall energy has no contribution from nearest neighbor exchange or double exchange. (c) Whatever the arrangement is, the angle Θ between neighboring units and the relative saturation m of each of them is still given by the formulas of Secs. II and III and the lower transition point T_1 is always observable.

Finally, we would like to mention the possible extension of all the above considerations to more complicated systems of mixed valency such as those derived from MnSe (rocksalt structure) or CrSb (NiAs structure). The case of $Cr_{1-x}Mn_xSb$ has already been mentioned in Sec. III. The compound $Mn_{0.9}Li_{0.1}Se$[15] is known to show two transition points T_1 and T_C. It is ferromagnetic between T_1 and T_C, and antiferromagnetic (with a strong parasitic ferromagnetism) at lower temperatures. Conductivity data have not appeared, and from the few experimental results presently available it is not yet possible to decide whether the low T arrangement is canted or not. We stress the fact that for the simpler case considered here a material which is ferromagnetic at high temperatures always displays a strong moment even below T_1, the angle between sublattice magnetizations being smaller than 103°, as explained in Sec. III.

ACKNOWLEDGMENTS

It is a pleasure to thank Professor C. Kittel and Professor A. M. Portis for discussions on these and related matters, and P. Pincus for checking the calculations.

APPENDIX 1. LOW-FREQUENCY SPIN WAVES

We consider the antiferromagnet layer structure of Sec. II, and study small amplitude motions of the ionic spin systems around the two sublattice equilibrium arrangement. The z axis is taken parallel to the spin direction in the pure material. The y axis is parallel to the spontaneous moment. The components of a spin $\mathbf{S}_i$ located on the first sublattice will be written as

$$S_i^x = S a_{ix}$$

$$S_i^y = S[\cos(\Theta_0/2) + a_{iy}]$$

$$S_i^z = S \sin(\Theta_0/2)\left(1 - \frac{a_{ix}^2 + a_{iy}^2}{2\sin^2(\Theta_0/2)} - \frac{a_{iy}\cos(\Theta_0/2)}{\sin^2(\Theta_0/2)} - \frac{1}{8}\frac{a_{iy}^2\cos^2(\Theta_0/2)}{\sin^4(\Theta_0/2)}\right) \quad (54a)$$

where terms up to second order in a_x, a_y have been retained. For a spin $\mathbf{S}_j$ located on the second sublattice we shall put

[15] S. J. Pickart, R. Nathans, and G. Shirane, Bull. Am. Phys. Soc. 4, 52 (1959); R. R. Heikes, T. R. McGuire, and R. J. Happel, Jr., Bull. Am. Phys. Soc. 4, 52 (1959).

$$S_j^x = Sb_{jx}$$

$$S_j^y = S[\cos(\Theta_0/2) + b_{jy}]$$

$$S_j^z = -S\sin(\Theta_0/2)\left(1 - \frac{b_{jx}^2 + b_{jy}^2}{2\sin^2(\Theta_0/2)} - \frac{b_{jy}\cos(\Theta_0/2)}{\sin^2(\Theta_0/2)} - \frac{1}{8}\frac{b_{jy}^2\cos^2(\Theta_0/2)}{\sin^4(\Theta_0/2)}\right). \quad (54b)$$

From these formulas we compute the exchange energy $-\sum J_{ij}S^2$ as θ_{ij} up to second order in a and b. To get the double exchange energy, we make use of three approximations: (a) low-frequency approximation; the Zener carriers are at every instant in the ground state corresponding to the distortion (54). (b) Long wavelength approximation; the distortion in (54) is nearly homogeneous. At every lattice point we may think of the carriers as occupying the bottom of a band whose width corresponds to the local value of the spin distortion. (c) Electrical neutrality approximation; we assume that the density of carriers is not modulated by the spin wave. (a), (b), and (c) may be shown to be entirely correct for the low-frequency part of the spin wave spectrum. We may then write the total energy as a sum of two terms, related with intralayer and interlayer couplings respectively:

$$E = E_{\text{intra}} + E_{\text{inter}} \quad (55)$$

and get:

$$E_{\text{inter}} = |J|S^2 \sum_{ij} (a_{iy} + b_{jy})^2 \quad (56)$$

$$E_{\text{intra}} = J'' \sum_{i>j} \{(a_{ix} - a_{jx})^2 + [1/\sin^2(\Theta_0/2)](a_{iy} - a_{jy})^2\} \quad (57)$$

where

$$J'' = J' + \tfrac{1}{4}xb'. \quad (58)$$

Equations (56) and (57) show that the energy is of second order in a and b, as expected. The fact that E_{inter} depends only on the y components of the distortion is simply a consequence of the degeneracy illustrated on Fig. 1. The dependence of E_{inter} on b has been eliminated by making use of Eq. (9) for Θ_0. From the energy formulas we can derive an effective field $\mathbf{H}_i$ acting on each spin $\mathbf{S}_i$ (our special choice of independent variables does not change the vector product $H_i \times S_i$). Putting $a_{ix} = A_x e^{i(\mathbf{k}\cdot\mathbf{R}_i + \omega t)}$, etc., we get finally:

$$\begin{aligned}
i\hbar\omega A_x &= [2J'/\sin(\Theta_0/2)](\gamma_0' - \gamma_k')A_y + 2J\sin(\Theta_0/2)(\gamma_0 A_y + \gamma_k B_y) \\
i\hbar\omega A_y &= -2J'\sin(\Theta_0/2)(\gamma_0' - \gamma_k')A_x \\
i\hbar\omega B_x &= -[2J'/\sin(\Theta_0/2)](\gamma_0' - \gamma_k')B_y - 2J\sin(\Theta_0/2)(\gamma_0 B_y + \gamma_k A_y) \\
i\hbar\omega B_y &= 2J'\sin(\Theta_0/2)(\gamma_0' - \gamma_k')B_x.
\end{aligned} \quad (59)$$

The secular equation derived from (59) is

$$\begin{aligned}
(\hbar\omega)^4 - 2(\hbar\omega)^2[2J''(\gamma_0' - \gamma_k') &+ 2|J|\sin^2(\Theta_0/2)\gamma_0]2J''(\gamma_0' - \gamma_k') \\
&+ (2J'')^2(\gamma_0' - \gamma_k')^2[2J''(\gamma_0' - \gamma_k') \\
&+ 2|J|\sin^2(\Theta_0/2)(\gamma_0 - \gamma_k)] \\
&\times 2|J|\sin^2(\Theta_0/2)(2\gamma_0) = 0.
\end{aligned} \quad (60)$$

For small k (which is the only case where our approximations are meaningful) the solutions are

$$\begin{aligned}
(\hbar\omega_1)^2 &= 8\gamma_0|J|J''\sin^2(\Theta_0/2)(\gamma_0' - \gamma_k') \\
(\hbar\omega_2)^2 &= 2J''(\gamma_0' - \gamma_k')[2J''(\gamma_0' - \gamma_k') + 2|J|\sin^2(\Theta_0/2)(\gamma_0 - \gamma_k)].
\end{aligned} \quad (61)$$

In the first branch ω is proportional to k (as it is in antiferromagnets), and in the second it is proportional to k^2 (as it is in ferromagnets). It is of interest to observe that both branches collapse when the intralayer coupling J'' vanishes.

APPENDIX 2. EXPANSION OF $\cos\theta/2$ IN TERMS OF LEGENDRE POLYNOMIALS $P_l(\cos\theta)$

We are interested in the coefficients A_l of Eq. (22). They are given by

$$\begin{aligned}
A_l &= \frac{2l+1}{2}\int_0^\pi P_l(\cos\theta)(\cos\theta/2)\sin\theta d\theta \\
&= \frac{2l+1}{2\sqrt{2}}\int_1^1 P_l(u)(1+u)^{\frac{1}{2}}du.
\end{aligned} \quad (62)$$

These integrals may be derived from the generating function

$$\frac{1}{(1-2uh+h^2)^{\frac{1}{2}}} = \sum_l h^l P_l(u) \quad (63)$$

by writing:

$$\int_{-1}^1 du\, y = 2\sqrt{2}\sum_l h^l \frac{A_l}{2l+1} \quad (64)$$

where $y^2 = [(1+u)/(1-2uh+h^2)]$. Equation (64) can be integrated by parts and yields

$$\frac{1}{2h}\left[h - 1 + (1+h)^2\frac{\tan^{-1}(h^{\frac{1}{2}})}{h^{\frac{1}{2}}}\right] = 2\sum_l \frac{A_l}{2l+1}h^l. \quad (65)$$

By expanding the left-hand side and identifying coefficients of h^l on both sides we get Eq. (23).

APPENDIX 3. LONG-RANGE PART OF A LOCAL SPIN DISTORTION

We choose to deal here with the simple example already used in the first part of Sec. IV (simple cubic alternating antiferromagnet with only one bond perturbed, between atoms 1 and 2). It was shown there that the spins S_1 and S_2 rotated by angles ϵ and $-\epsilon$

from their initial (antiparallel) orientations. We now consider the smaller deflections ϵ_i (assumed all in the same plane) which are found on the other magnetic sites ($i \neq 1, 2$). All these sites are submitted only to exchange forces, and for small ϵ_i then equilibrium conditions take the simple form

$$\gamma_0 \epsilon_i = \sum_j{}' \epsilon_j \tag{66}$$

where the sum $\sum_j{}'$ is extended to all 6 nearest neighbors of site i, and

$$\gamma_k = \sum_j{}' e^{i\mathbf{k}\cdot\mathbf{R}_{ij}}. \tag{67}$$

[Note that γ_k, defined here by (67), for an alternating antiferromagnet, is different from the γ_k defined in Sec. II, for a layer antiferromagnet.] The solution of Eq. (66) which exhibits the required values on the perturbed sites is easy to express in terms of the Green's function

$$\Gamma_{lm} = A \sum_k \frac{\gamma_0}{(\gamma_0 - \gamma_k)} e^{i\mathbf{k}\cdot(\mathbf{R}_l - \mathbf{R}_m)} \tag{68}$$

where the sum $\sum_k$ is extended over the first Brillouin zone and where A is a normalization factor chosen to give $\Gamma_{ll} = 1$.

$$A^{-1} = \sum_k \frac{\gamma_0}{\gamma_0 - \gamma_k}. \tag{69}$$

The numerical value of A is 0.65947.[16] The quantity Γ_{lm} considered as a function of l (or m) satisfies Eq. (66) except when $l = m$. It describes the deflection of spin $\mathbf{S}_m$ when one spin $\mathbf{S}_l$ has been submitted to a prescribed deflection. Γ_{lm} is a slowly decreasing function of $|\mathbf{R}_l - \mathbf{R}_m|$. It has the following asymptotic form

$$\Gamma_{lm} = (3A/2\pi)a/|\mathbf{R}_l - \mathbf{R}_m| \tag{70}$$

where a is the length of the cube edge. Let us first consider the case where all deflections are small, even on the perturbed sites (1) and (2). Then the complete solution of Eq. (66) satisfying the boundary condition is

$$\epsilon_i = \epsilon(\Gamma_{1i} - \Gamma_{2i})/(1 - \Gamma_{12}). \tag{71}$$

This may still be simplified by observing that $1 - \Gamma_{12} = A$.

We now discuss a few important features of this result. (1) The angles ϵ_i for (i) different from (1) and (2) are substantially smaller than ϵ. Consider for instance the sites (i') which are nearest neighbors of (1), (2) being excluded. The average deflection of these sites is $\bar{\epsilon}_{(i')} = \frac{1}{5}\sum_{i'} \epsilon_{i'}$. By manipulating the Γ functions, one easily shows from (71) that

$$|\bar{\epsilon}_{i'}| = \tfrac{1}{5}\epsilon. \tag{72}$$

This explains *a posteriori* why the rigid field approximation used in Sec. IV is a good starting point. (2) The deflection ϵ_i is proportional to $\Gamma_{1i} - \Gamma_{2i}$. At long distances from the impurity center, Γ_{1i} is similar to the potential of a point charge, as shown by Eq. (70) and $\Gamma_{1i} - \Gamma_{2i}$ behaves like the potential of a dipole. This gives rise to a very specific neutron diffraction pattern, which we now compute.

For small ϵ_i the scattering amplitude for a scattering vector $\mathbf{q}$ is, apart from polarization factors and normalization constants:

$$a(\mathbf{q}) = \sum_i \epsilon_i \sigma_i e^{i\mathbf{q}\cdot\mathbf{R}_i}, \tag{73}$$

where $\sigma_i = \pm 1$ depending on the sublattice to which (i) belongs. Equation (73) takes into account only the scattering due to the spin distortion. (The amplitude due to the ordered structure vanishes except on Bragg peaks, which we discard.) Equation (73) may be transformed by making use of the solution (71) and of the defining equation (68) for the Γ_{lm}. Finally we compute $|a(\mathbf{q})|^2$, take an average over the three possible orientations of the pair (12) and multiply by the number Nx of modified bonds in the crystal. The result is

$$\langle |a(\mathbf{q})|^2 \rangle = \frac{2Nx\epsilon^2\gamma_0}{\gamma_0 - \gamma(\mathbf{q} - \boldsymbol{\tau}_s)} \tag{74}$$

where $\boldsymbol{\tau}_s$ is the scattering vector corresponding to a superlattice line [they are all equivalent here; for instance we may take $\boldsymbol{\tau}_s = (\pi/a, \pi/a, \pi/a)$]. We see that the distortion gives rise to a diffuse scattering around the magnetic peaks of the unperturbed matrix. When $\mathbf{q} - \boldsymbol{\tau}_s$ is small (74) takes the limiting form

$$|a(\mathbf{q})|^2 = 12Nx\epsilon^2/(|\mathbf{q} - \boldsymbol{\tau}_s|^2 a^2). \tag{75}$$

We now discuss the parasitic scattering, due to thermal distortions (spin waves) which may prevent observation of this effect. It often happens that this scattering is also concentrated around the magnetic peaks.[17] However, the spin-wave effects may be made diffuse by a suitable geometrical arrangement, as we shall now show. The parasitic scattering is due to neutrons, of initial wave vector $\mathbf{k}_0$, emitting or absorbing a spin wave ($\mathbf{q}$). Energy and "momentum" conservation require that

$$\hbar\omega_{\mathbf{q}} = \pm(\hbar^2/2M)[(\mathbf{q} + \mathbf{k}_0)^2 - k_0^2] \tag{76}$$

where M is the neutron mass and $\omega_{\mathbf{q}}$ the spin wave frequency, which is given by

$$\omega_{\mathbf{q}} = c|\mathbf{q} - \boldsymbol{\tau}_s| \tag{77}$$

when $\mathbf{q}$ is close to $\boldsymbol{\tau}_s$. The constant $c = [(12|J|Sa)/\sqrt{3}\hbar]$ is the velocity of the spin wave. If the velocity of the ingoing neutron $\hbar k_0/M$ is smaller than c, Eqs. (76) and (77) have no solution in the vicinity of $\mathbf{q} = \boldsymbol{\tau}_s$. The inelastic scattering is then distributed on a very wide surface in $\mathbf{q}$ space, and shows no anomaly near the magnetic peaks; it does not prevent the observation of the scattering due to static spin distortions [the latter

[16] M. Tickson, J. Research Natl. Bur. Standards **50**, 177 (1953).

[17] R. J. Elliott and R. D. Lowde, Proc. Roy. Soc. (London) **A230**, 46 (1955).

being indeed singular, as shown by Eq. (75)]. On the other hand k_0 must not be too small. We get superlattice reflections only if $2k_0 > \tau_s$. Both requirements may be satisfied if $\tau_s < 2Mc/\hbar$. Expressing J in terms of the Néel temperature of the pure material by the approximate relation $4|J|S(S+1) = k_B T_N$ we find that this condition may be written

$$\rho = \frac{k_B T_N M a^2}{(S+1)\hbar^2} > \frac{\pi}{2}. \tag{78}$$

Taking $a = 3$ A, $T_N = 80°$K and $S = \frac{3}{2}$ we get $\rho = 7$, so that the inequality (78) seems easy to satisfy. In our example, the experiment is feasible with neutron wavelengths $2\pi/k_0$ between 1.5 and 3 A.

Our formula (71) was restricted to cases where the deflection $\epsilon = \epsilon_1 = -\epsilon_2$ on the perturbed sites was small. In practice this is not the case, and (71) does not apply. However, it is always a good approximation to assume that all deflections other than ϵ_1 and ϵ_2 are indeed small. It may then be shown that the simple solution (71) is still acceptable provided that we replace ϵ by $\sin\epsilon$. With this slight modification all the later formulas also retain their validity.

PHYSICAL REVIEW VOLUME 118, NUMBER 1 APRIL 1, 1960

Electron-Hydrogen Scattering at Low Energies

TAKASHI OHMURA* AND HARUKO OHMURA†
Division of Pure Physics, National Research Council, Ottawa, Canada
(Received October 23, 1959)

The effective range in the singlet electron-hydrogen system has been evaluated as 2.646±0.004 atomic units by using the asymptotic amplitude of the 202-parameter H^- wave function of Pekeris. This value of the effective range, together with the value of the electron affinity of H^-, determines the scattering length in the singlet system as 6.167 atomic units. The effective range in the triplet system is calculated to be 1.219 atomic units by a Hartree-Fock approximation. It is shown that the effective-range approximation is very good for all energies at which only elastic scattering is allowed. The photo-ionization of H^- is briefly discussed on the basis of the effective-range theory.

I. INTRODUCTION

THE low-energy scattering of an electron by a hydrogen atom is described by four parameters, the scattering lengths a_+ and a_- and the effective ranges r_{0+} and r_{0-}. + refers to the singlet system and − the triplet system. The s phase shift is given, in the so-called effective range approximation, by

$$k\cot\eta_\pm = -(1/a_\pm) + (r_{0\pm}/2)k^2 + O(k^4). \tag{1a}$$

The s scattering in the singlet system is also described by the electron affinity ($\gamma^2/2$) of H^- and by the effective range ρ at the ion state.

$$k\cot\eta_+ = -\gamma + \tfrac{1}{2}\rho(\gamma^2+k^2) + O[(\gamma^2+k^2)^2]. \tag{1b}$$

Detailed variational calculations for the phase shifts have been carried out by Massey and Moiseiwitsch[1] among others[2] by taking into account the effect of the polarization. It has been found[3] recently that Massey-Moiseiwitsch's results are well reproduced by the effective range approximation (1a) and (1b) even for quite high energies, ($k^2 \lesssim 1$). The most reliable values hitherto obtained for the low-energy parameters may be summarized as follows:

$$a_+ = 6\text{—}7,^{3,4} \qquad a_- = 2.33\text{—}2.34,^{4,5}$$
$$\rho = 2.4_4\text{—}2.6,^{3} \qquad r_{0-} = 0.8\text{—}1.3.^{6,5}$$

The atomic units are used throughout this paper.

The effective range ρ of the singlet system will be evaluated in II by using the asymptotic amplitude of the Pekeris wave function for the negative hydrogen ion state with 202 adjustable parameters. In III the triplet effective range will be computed in the so-called exchange approximation. In IV a discussion is given of the comparison with Massey and Moiseiwitsch's result and the experimental data, and of the bound-free transition of the negative hydrogen ion.

II. EVALUATION OF ρ BY THE PEKERIS WAVE FUNCTION

Recently Pekeris[7] has succeeded in obtaining very accurate wave functions for the ground states of two-

* National Research Council Postdoctorate Fellow on leave of absence from Department of Physics, University of Tokyo, Tokyo, Japan.
† National Research Council Guest Worker on leave of absence from Department of Physics, University of Tokyo, Tokyo, Japan.
[1] H. S. W. Massey and B. L. Moiseiwitsch, Proc. Roy. Soc. (London) **A205**, 483 (1951).
[2] H. S. W. Massey, Revs. Modern Phys. **28**, 199 (1956), and the papers cited there.
[3] T. Ohmura, Y. Hara, and T. Yamanouchi, Progr. Theoret. Phys. (Kyoto) **22**, 152 (1959).
[4] M. J. Seaton, Proc. Roy. Soc. (London) **A241**, 522 (1957).
[5] T. Ohmura, Y. Hara, and T. Yamanouchi, Progr. Theoret. Phys. (Kyoto) **20**, 82 (1958).
[6] S. Borowitz and H. Greenburg, Phys. Rev. **108**, 716 (1957).
[7] C. L. Pekeris, Phys. Rev. **112**, 1649 (1958).